

Pyrometry for Turbine Applications in the Presence of Reflection and Combustion

E. Suarez*

Pratt & Whitney, West Palm Beach, Florida 33410

Nomenclature

E = radiant power
 T = temperature

Subscripts

c = reflection corrected
 l = long wavelength band
 m = mid wavelength band
 r = reflected radiation
 s = short wavelength band

Introduction

IN the turbine environment the pyrometer output temperature must be corrected for reflected radiation from the combustor and flame in the field of view. This Note describes on-line correction algorithms using triple-band pyrometry and data sorting.

Correction for Combustion Interference in the Field of View

Flame in the field of view overwhelms the radiation emitted by the turbine blade making the pyrometer unusable. Since the occurrence of flame is random and always drives the temperature signal high, flame-free data is obtained by continuously sampling the same point on the blade surface and discarding the high temperature values while retaining the low for further comparison. The algorithm accounts for variations in engine speed and the level of signal noise.

Data processing consists of sampling temperature signals and a reference revolution pulse that provides turbine rotor position. A sufficient number of temperature points are acquired to cover at least one rotor revolution. The first data set becomes the baseline revolution to which data points in successive revolutions will be compared. The number of points contained in a rotor revolution must stay constant to represent the same location on the turbine blade airfoil. Even at constant engine speed there is enough variation in rotational speed to require adjustment. To adjust a revolution, the difference in the number of data points between the revolution and the baseline are proportionally inserted or deleted.

Each new set of uncorrected temperatures is compared to the baseline set. The baseline set is replaced if the difference between the baseline value and the new value is greater than the noise level. If the difference is within the noise, the new value is weight-averaged to the values in the baseline. Figure 1 shows the temperature profile for a turbine revolution after correction for flame. After the flame is eliminated from the data, the temperatures are corrected for reflection.

Correction for Combustor Reflection

The spectral variability and high level of reflected radiation present in the turbines of modern jet engines has exceeded

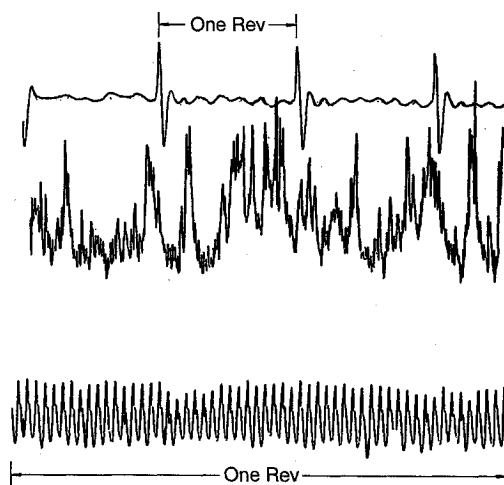


Fig. 1 Pyrometer signal with flame interference and after correction.

the correction limit of techniques such as the dual spectral area pyrometer (DSAP). In DSAP technique¹⁻³ the requirement of constant spectral distribution for the reflected radiation leads to significant errors. Using three wavelength bands, the triple spectral area pyrometer (TRISAP) reduces the error by calculating the ratio temperature of the reflected component. Figure 2 compares this error for DSAP and TRISAP as a function of reflection level for a $\pm 200^\circ\text{F}$ fluctuation in combustor radiance temperature. Reflection levels in development engines at high power reach 70% of the input signal. At this level the DSAP method exceeds the accuracy requirement of $\pm 25^\circ\text{F}$.

The TRISAP algorithm is based on the fact that corrected temperatures calculated using any two bands will be equal if the correct spectral ratio for the reflection component is used. If the temperatures disagree, the spectral ratio is increased or decreased depending on the magnitude and sign of the temperature difference until the corrected temperatures converge.

The three spectral bands were selected to provide a clear window through the combustion gases, adequate signal-to-noise, and sensitivity to the reflected component. The spectral bands being used are

short band = $0.40\text{--}0.85\ \mu\text{m}$
 midband = $0.85\text{--}1.00\ \mu\text{m}$
 long band = $1.00\text{--}1.80\ \mu\text{m}$

Signals E_s , E_m , and E_l are used to calculate two corrected temperatures, one using the middle and short band, the other using the long and middle band. The reflection component is removed by the following expressions:

$$E_{ms} = E_m - (E_{mr}/E_{sr})E_s \quad (1)$$

$$E_{lm} = E_l - (E_{lr}/E_{mr})E_m \quad (2)$$

The quantity in parenthesis is the spectral ratio for the combustor reflection in the measurement bands. For given values of E_{ms} and E_{lm} , the corrected blade temperatures T_{cms} and T_{clm} remain only functions of the spectral ratios. The difference between corrected temperatures T_{cms} and T_{clm} is used to verify and adjust the values for the spectral ratios. If T_{cms} is greater than T_{clm} , the selected values for spectral ratios are low, which implies that the actual ratio temperature or black-body temperature that matches the spectral distribution for the combustor is less than the assumed value. Conversely, if T_{cms} is less than T_{clm} the selected values for spectral ratios are high, which implies that the actual ratio temperature for combustor emission is higher. Iterations adjusting the value for

Presented as Paper 93-2374 at the AIAA/SAE/ASME/ASME 29th Joint Propulsion Conference and Exhibit, Monterey, CA, June 28-30, 1993; received Sept. 1, 1993; revision received March 4, 1994; accepted for publication March 8, 1994. Copyright © 1993 by the American Institute of Aeronautics and Astronautics, Inc. All rights reserved.

*Development Engineer, Instrumentation Department.

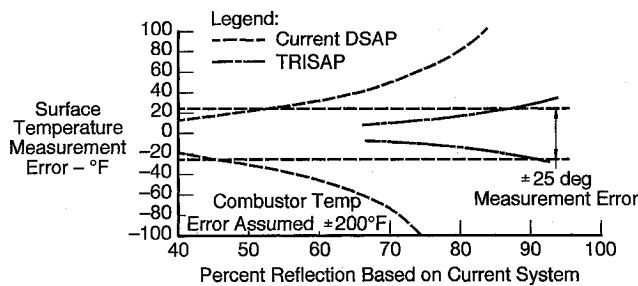


Fig. 2 Error due to variability of combustor radiance temperature.

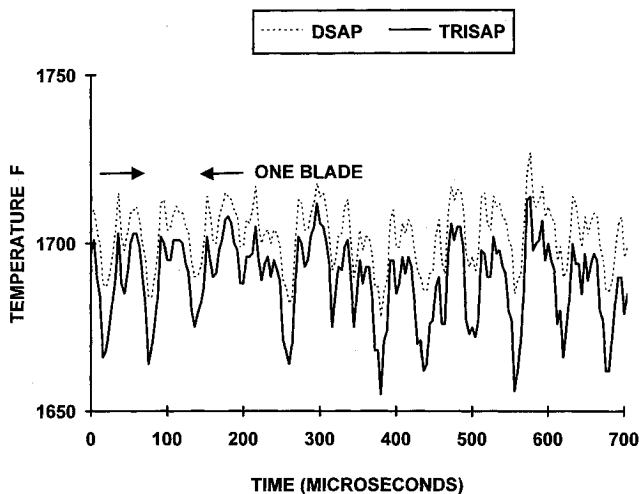


Fig. 3 Comparison of TRISAP and DSAP methods.

spectral ratios are performed until the temperatures agree within a predetermined limit selected to provide acceptable measurement uncertainty.

Figure 3 shows the results of simultaneous engine tests of the prototype TRISAP and a DSAP. The test objectives were to verify that there was no radiant contribution from the gas path in the long wavelength band and validate operability of the TRISAP system. In this test the reflection level averaged 56%, the average reflection ratio temperature calculated by the TRISAP was 4044°F, and DSAP used a conventional constant temperature correction of 4500°F. Under these conditions the DSAP will not correct the data sufficiently, resulting in erroneously high temperatures as shown in the plot.

Conclusions

Data sorting and triple wavelength pyrometry have been applied successfully to obtain on-line correction for flame in the field of view and levels of reflection exceeding 70% of input signal from a spectrally variable source. These methods provide cost-effective temperature data for turbine blade cooling development in the harsh and complex radiative environment of the first turbine, where other methods like the DSAP and thermographic phosphors have not been successful.

References

- ¹Atkinson, W. H., and Strange, R. R., "Pyrometer Temperature Measurements in the Presence of Reflected Radiation," American Society of Mechanical Engineers, ASME Paper 76-HT-74, New York, Aug. 1976.
- ²Atkinson, W. H., and Strange, R. R., "Turbine Pyrometer for Advanced Engines," AIAA Paper 87-2011, July 1987.
- ³Suarez, E., and Przireble, H. R., "Pyrometry for Turbine Blade Development," *Journal of Propulsion and Power*, Vol. 6, No. 5, 1990, pp. 584-589.

Stationkeeping with Two-Way Electromagnetic Launchers

Gerald David Nordley*
Sunnyvale, California 94089

Nomenclature

- D = parabolic eccentric anomaly, rad
- E = eccentric anomaly, rad
- e = orbital eccentricity, dimensionless
- F = effective thrust, N
- G = universal gravitational constant, $\text{N-m}^2/\text{kg}^2$
- H = hyperbolic eccentric anomaly, rad
- h = specific angular momentum, N-m-s/kg or m^2/s
- M = mass of primary body, kg
- m = reaction mass, kg
- p = semilatus rectum, m
- ρ = momentum, kg-m/s
- r = radius from the center of the primary body, m
- T = time of flight from periapsis, s
- v = velocity, m/s
- ϵ = specific kinetic energy, J/kg
- θ = true anomaly, rad
- ϕ = flight-path angle (from horizon), rad
- ω = angular velocity of the primary-secondary system, rad/s

Subscripts

- m = refers to the reaction mass
- $'$ = quantities measured in the launcher reference frame, as in v' for launch velocity
- 1 = refers to the launch point
- 2 = refers to the recovery point

Introduction

SERIOUS consideration of electromagnetic launchers (EML) for propulsion in space goes back to Clarke's¹ 1950 proposals for EML to launch payloads from the moon and Space Stations. O'Neill² provides a good summary of much of the early work and ideas in this field.

With modern computer-controlled attitude and velocity control systems on the payload, it is possible, in principle, for some kinds of EML to decelerate as well as launch payloads. A recent contribution by Forward³ referred to a suggestion in an unpublished novel by the author to use an EML to keep a Space Station at the L1 point of the Earth-moon orbit from drifting inward-outward (the L1 point is stable with respect to E-W or N-S perturbations).

This involved sending a mass from the L1 point on a classic "free return" trajectory and catching it on the way back. This trajectory was used (in essence) by Jules Verne⁴ and more recently by the Apollo 13 mission. It forms a "figure" eight shape if viewed in a frame of reference rotating with the same angular velocity as the moon (Fig. 1a). In this frame, if a mass is sent toward the moon, the EML is pushed toward Earth, both when sending the mass out and when catching it on its return. If the mass is sent toward the Earth and back on a related trajectory, the EML is pushed toward the moon.

Analysis

Figure one shows the basic architecture of the system in frame of reference rotating with the mean angular velocity of

Received July 26, 1992; revision received Feb. 17, 1994; accepted for publication March 18, 1994. Copyright © 1994 by the American Institute of Aeronautics and Astronautics, Inc. All rights reserved.

*Consultant and Writer, Major, U.S. Air Force, retired, 1238 Prescott Avenue. Member AIAA.